Journal of Magnetic Resonance 378 (2025) 107926

Contents lists available at ScienceDirect

Journal of Magnetic Resonance

journal homepage: www.elsevier.com/locate/jmr

Towards complete suppression of diagonal peaks in solid-state MAS NMR homonuclear chemical shift correlation spectra

Shengyu Zhang [a,f], Yuchen Li [a], Yansheng Ye [b,c,d], Fang Tian [b], Xinhua Peng [a,f,*], Riqiang Fu [e,*]

[a] Laboratory of Spin Magnetic Resonance, School of Physical Sciences, Anhui Province Key Laboratory of Scientific Instrument Development and Application, University of Science and Technology of China, Hefei 230026, China
[b] Department of Molecular and Precision Medicine, Pennsylvania State University, Hershey, PA 17033, USA
[c] State Key Laboratory of Magnetic Resonance Spectroscopy and Imaging, National Center for Magnetic Resonance in Wuhan, Wuhan Institute of Physics and Mathematics, Innovation Academy for Precision Measurement Science and Technology, Chinese Academy of Sciences, Wuhan 430071, China
[d] University of Chinese Academy of Sciences, Beijing 100049, China
[e] National High Magnetic Field Laboratory, 1800 E Paul Dirac Dr., Tallahassee, FL 32310, USA
[f] Hefei National Laboratory, University of Science and Technology of China, Hefei 230088, China

ARTICLE INFO

Keywords:
Diagonal peak suppression
Spin echo
^{13}C–^{13}C chemical shift correlation spectra
Solid-state MAS NMR
Data processing

ABSTRACT

The feasibility of applying the spin-echo based diagonal peak suppression method in solid-state MAS NMR homonuclear chemical shift correlation experiments is demonstrated. A complete phase cycling is designed to generate sine- and cosine-modulations of the chemical shift difference between the spin-diffused signals, enabling the quadrature detection in the indirect dimension. Meanwhile, all signals not involved in polarization transfer are refocused at the center of the indirect dimension. A data processing algorithm is developed to extract and suppress these spin-echo refocused signals without affecting nearby spin-diffused cross peaks. The processed spectrum is then converted into a conventional two-dimensional homonuclear chemical shift correlation spectrum, free of diagonal peaks. The effectiveness of this method is illustrated using a uniformly ^{13}C-labeled Fmoc-leucine sample and a sample of human Atg8 homolog LC3B, directly conjugated to the amino headgroup of phosphatidylethanolamine (PE) lipids in liposomes.

1. Instruction

In recent decades, solid-state magic-angle-spinning (MAS) NMR has rapidly emerged as a powerful technique for studying insoluble proteins. Among the most routine experiments, ^{13}C–^{13}C homonuclear correlation spectroscopy provides essential long-range carbon-carbon distance restraints for the structural determination of uniformly ^{13}C and ^{15}N labeled proteins. However, strong autocorrelated signals, or diagonal peaks, are inevitably present and typically more intense than cross peaks in ^{13}C–^{13}C homonuclear chemical shift correlation NMR spectra. These diagonal peaks arise not only from the ^{13}C-labeled proteins under investigation but also from natural abundance ^{13}C signals in membrane-mimetic environments and lipids, which are essential and integral components of membrane proteins. While cross peaks contain valuable information about distance restraints among nuclei, the strong diagonal peaks provide little additional information and often obscure nearby weak cross peaks. Additionally, the intense diagonal signals often cause t_1-noise and other artifacts in the indirect dimension [1,2]. Therefore, suppressing diagonal peaks in the homonuclear correlation spectra is critical for revealing these useful but buried cross peaks for structural studies.

Double-quantum (DQ) coherence is known to be effective for selecting coupled spins while removing all uncoupled signals, such as those from natural abundance isotopes or from membrane-mimetic environments and lipids that support membrane proteins [3–6]. For instance, the DQ filtered correlation spectroscopy (DQF-COSY) can be used to obtain correlations between coupled spins in a system, effectively eliminating unwanted background signals from uncoupled spins [7], but their diagonal peaks remain. INADEQUATE [7] is another method utilizing DQ filtering to obtain the connectivity between coupled spins in DQ-SQ (single-quantum) correlation spectra, while also suppressing those unwanted background signals from uncoupled spins.

* Corresponding authors.
E-mail addresses: xhpeng@ustc.edu.cn (X. Peng), rfu@magnet.fsu.edu (R. Fu).

https://doi.org/10.1016/j.jmr.2025.107926
Received 30 March 2025; Received in revised form 2 June 2025; Accepted 24 June 2025
Available online 25 June 2025

Table 1
Phase cycling used in Fig. 1c to generate the pure sine and cosine modulations of the chemical shift difference between two spin-diffused spins.

To generate sine modulation	φ_1	1 3
	φ_2	1 1 1 1 3 3 3 3 2 2 2 2 0 0 0 0
	φ_3	1 1 1 1 1 1 1 1 0 0 0 0 0 0 0 0 3 3 3 3 3 3 3 3 2 2 2 2 2 2
	φ_4	2 2 0 0
	φ_5	0
	Receiver	1 3 3 1 3 1 1 3 1 3 3 1 3 1 1 3 3 1 1 3 1 3 3 1 3 1 1 3 1 1 3 3 1 3 1 1 3 3 1
To generate cosine modulation	φ_1	1 3
	φ_2	1 1 1 1 3 3 3 3 2 2 2 2 0 0 0 0
	φ_3	1 1 1 1 1 1 1 1 0 0 0 0 0 0 0 0 3 3 3 3 3 3 3 3 2 2 2 2 2 2
	φ_4	1 1 3 3
	φ_5	1
	Receiver	0 2 2 0 2 0 0 2 0 2 2 2 0 2 0 0 2 2 0 0 2 0 2 0 2 2 0 2 0 0 2 0 2 2 0 2 0 0 2 0

Here 0, 1, 2, and 3 represent the phase direction of x, y, −x, and −y, respectively.

This method is very effective for those spins that are in close approximate, even if their chemical shifts are identical, but not for those spins that are in a longer range, thus incapable of obtaining long-range distance restraints between the labeled ^{13}C sites necessitated for NMR protein structural elucidations. Through-space ^{13}C–^{13}C spin diffusion [8–11] remains to be an effective way to obtain such long-range distance restraints.

Recently, Xue et al. [12] utilized different signals from cross polarization (CP) steps in each scan, i.e., the CP-transferred signals that participate in spin diffusion process through ^{1}H and the CP-non-transferred signals that do not involve in spin diffusion. Subtracting these two signals leads to partial attenuation of the diagonal peaks without affecting the sensitivity of the cross peaks. On the other hand, based on the spin-echo based diagonal peak suppression (DIPS) method proposed in solution NMR [13], a sophisticated phase cycling scheme [14] has been used in solid state MAS NMR spectroscopy to select a sine modulation of the chemical shift difference between the spin-diffused signals in the indirect (i.e., t_1) dimension, while completely suppressing all autocorrelated peaks. Fourier transform of the sine-modulated signals results in a spectrum with pairs of positive and negative peaks positioning symmetrically at the chemical shift difference between the correlated sites with respect to the spectral center in the indirect dimension. This spectrum can be reconstructed into a standard chemical shift correlation spectrum free of diagonal peaks after a post-processing procedure [15]. However, the presence of the positive and negative peaks may lead to signal cancellation from different pairs of the spin-diffused signals, particularly in crowded 2D spectra of proteins.

Here, we revisit the spin-echo based method and design another set of phase cycling to select a cosine modulation of the chemical shift difference between spin-diffused signals in the t_1 dimension. As a result, quadrature detection of the chemical shift difference between the spin-diffused signals in the t_1 dimension is achieved through the hypercomplex method by combining both sine and cosine modulations. This approach ensures that all spin-diffused cross peaks in the resulting spectrum are positive, while all autocorrelated signals are refocused, as in the standard spin echo experiment, and appear at the zero-frequency along the t_1 dimension. Furthermore, an algorithm for a post data processing protocol is developed to remove these spin-echo refocused signals, resulting in complete removal of diagonal peaks in the reconstructed spectra. A uniformly ^{13}C, ^{15}N labeled Fmoc-valine sample and a sample of human Atg8 homolog LC3B, directly conjugated to the amino headgroup of phosphatidylethanolamine (PE) lipids in liposomes, were used to demonstrate the suppression of diagonal peaks in the ^{13}C–^{13}C correlation spectra and to evaluate the performance of this method in comparison with the standard ^{13}C–^{13}C correlation spectra.

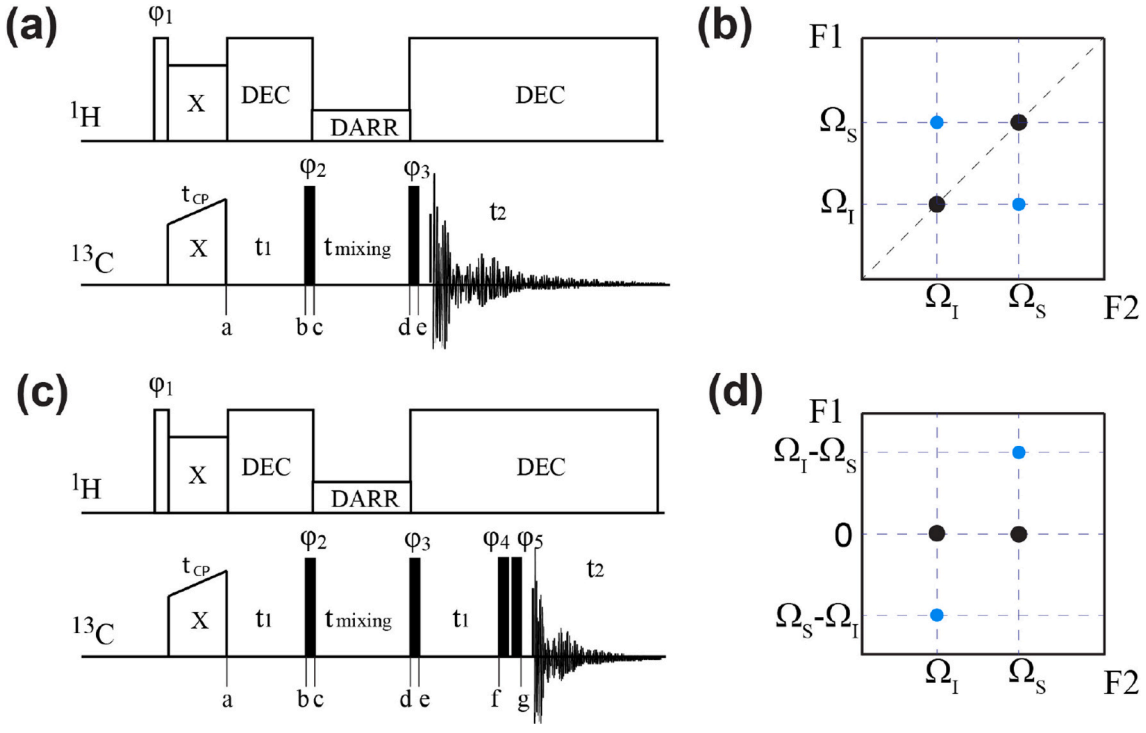

Fig. 1. (a) Pulse sequence used for standard ^{13}C–^{13}C correlation experiments in solid-state NMR and (b) its resonance pattern in a 2D spectrum. (c) Pulse sequence for diagonal peak suppression scheme in solid-state NMR and (d) its 2D resonance pattern. Here, DARR refers to dipolar assisted rotational resonance irradiation during the mixing time for enhancing ^{13}C–^{13}C spin diffusion; "DEC" represents decoupling irradiation. The open rectangle in ^{1}H channel and solid rectangles in ^{13}C channel stand for 90° pulses. While Ω_I and Ω_S represent two ^{13}C signals that correlated with each other. The complete phase cycling designed to select the chemical shift difference terms is listed in Table 1.

2. Methodology

Fig. 1a shows the pulse sequence for standard ^{13}C–^{13}C chemical shift correlation experiments in solid-state NMR. After enhanced through cross polarization from ^{1}H, the ^{13}C magnetization evolves under high-power ^{1}H decoupling for a period of time t_1, followed by a 90° pulse to flip the magnetization from the xy plane to the z-axis. Along the longitudinal axis, the ^{13}C–^{13}C spin diffusion is enhanced through dipolar assisted rotational resonance (DARR) [9,16] during a mixing time of t_{mixing} to transfer the ^{13}C magnetization from one site to others. The magnetization is brought back to the xy plane at the end of the mixing time by the second 90° pulse for detection under high-power ^{1}H decoupling. Here we use an *I*–*S* two-spin system for simplicity to illustrate the correlation between the *I* and *S* spins where their respective chemical shifts are Ω_I and Ω_S. Assuming no *J*-coupling is present between these two spins, the *I* and *S* magnetizations evolved at different stages in the pulse sequence can be described as follows:

After cross polarization, we have

(a): $I_X + S_X$

When evolving for the t_1 period under their respective frequencies, these magnetizations become

(b): $I_X\cos(\Omega_I t_1) + I_Y\sin(\Omega_I t_1) + S_X\cos(\Omega_S t_1) + S_Y\sin(\Omega_S t_1)$

Applying a $90°_y$ (i.e. $\varphi_2 = y$) to flip I_X and S_X components to the z-axis, we obtain

(c): $-I_Z\cos(\Omega_I t_1) + I_Y\sin(\Omega_I t_1) - S_Z\cos(\Omega_S t_1) + S_Y\sin(\Omega_S t_1)$.

During t_{mixing}, the magnetizations along the z-axis are diffused between *I* and *S*, while the magnetizations remaining in the xy-plane will eventually be dephased (or suppressed through the phase cycling). Thus, we have

(d): $-(C_I I_X + C_{I\to S}S_X)\cos(\Omega_I t_1) - (C_S S_X + C_{S\to I}I_X)\cos(\Omega_S t_1)$.

Here, $C_{j\to k}$ is the transfer coefficient from *j* to *k* spin during the mixing time, while C_I and C_S stand for the self-transfer coefficients for the *I* and *S* spin over the mixing time, which depend on their spin-lattice relaxation times as well as the amount of magnetizations diffused away from *I* to *S* and from *S* to *I*, respectively. After the second 90°, the *I* and *S* spins evolve under their respective chemical shifts during the detection in the t_2 dimension, the observed signals can be represented, when using the quadrature detection in the t_1 dimension, by:

$$s(t1,t2) = C_I e^{-i\Omega_I t_1} e^{-i\Omega_I t_2} + C_{S\to I} e^{-i\Omega_S t_1} e^{-i\Omega_I t_2} + C_{I\to S} e^{-i\Omega_I t_1} e^{-i\Omega_S t_2} + C_S e^{-i\Omega_S t_1} e^{-i\Omega_S t_2} \quad (1)$$

Clearly, the C_I and C_S terms exhibit their own chemical shift modulations in both t_1 and t_2 dimensions, corresponding to the diagonal peaks after Fourier transform. In contrast, the $C_{I\to S}$ and $C_{S\to I}$ terms carry different chemical shift modulation in the t_1 and t_2 dimensions, leading to the cross peaks between the *I* and *S* spins, as illustrated in Fig. 1b.

The pulse sequence we designed to suppress diagonal peaks is shown in Fig. 1c. After the second 90° pulse, the evolution for another t_1 period generates time modulations for various frequencies: Ω_I, Ω_S, $\Omega_I + \Omega_S$, $\Omega_I - \Omega_S$, and 0 (i.e., $\Omega_I - \Omega_I$ or $\Omega_S - \Omega_S$). With two additional 90° pulses at the end of the second t_1 period, we can select either a sine or a cosine modulation for the chemical shift difference $\Omega_I - \Omega_S$, as detailed in Supplemental Information:

(sg): $C_{I\to S}S_Y\sin((\Omega_I - \Omega_S)t_1) + C_{S\to I}I_Y\sin((\Omega_S - \Omega_I)t_1)$

(cg): $C_I I_X + C_{I\to S}S_X\cos((\Omega_I - \Omega_S)t_1) + C_S S_X + C_{S\to I}I_X\cos((\Omega_S - \Omega_I)t_1)$

Therefore, with the hypercomplex method, the observed signals during the t_2 detection period are

$$s(t1,t2) = C_I e^{-i\Omega_I t_2} + C_{S\to I} e^{-i(\Omega_S - \Omega_I)t_1} e^{-i\Omega_I t_2} + C_{I\to S} e^{-i(\Omega_I - \Omega_S)t_1} e^{-i\Omega_S t_2} + C_S e^{-i\Omega_S t_2}. \quad (2)$$

Clearly, the C_I and C_S terms are independent of t_1, implying that the spin-echo refocused diagonal peaks appear at the zero-frequency in the t_1 dimension. While the spin-diffused $C_{I\to S}$ and $C_{S\to I}$ terms appear at the positions of their chemical shift differences in the F1 indirect dimension, representing the cross peaks between the *I* and *S* spins. Unlike the sine modulation of $\Omega_I - \Omega_S$ that leads to a pair of peaks positioning at the frequency of $\pm(\Omega_I - \Omega_S)$ with opposite signal intensities in the F1 dimension [14], this hypercomplex method allows to obtain all positive peaks with their distinct positions at $(\Omega_I - \Omega_S)$ and $(\Omega_S - \Omega_I)$, as illustrated in Fig. 1d. While the diagonal peaks are spin-echo refocused and should be symmetric with respect to the center in the F1 dimension. We refer this quadrature detected diagonal peak suppression DARR scheme as ^{QD}DIPS-DARR in the following discussion.

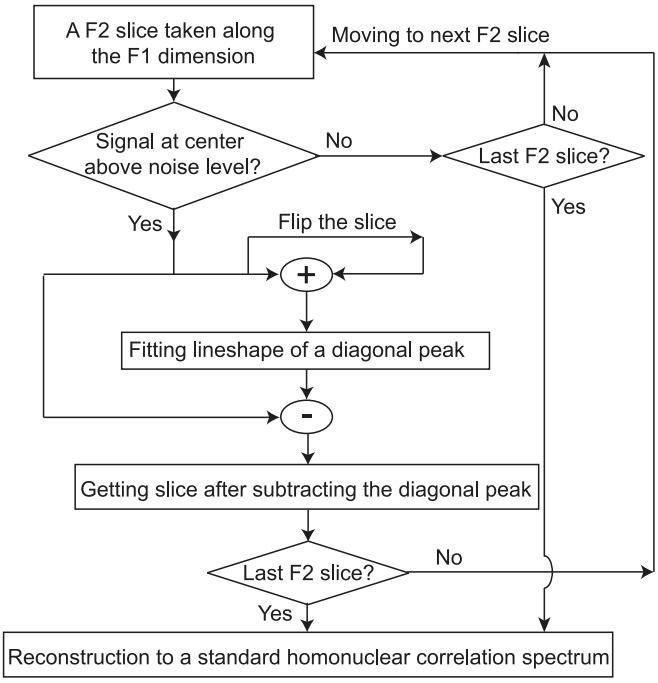

Fig. 2. Data processing flowchart to extract the symmetric spin-echo refocused diagonal peaks and subtract them from the ^{QD}DIPS-DARR spectrum.

The question is whether these spin-echo refocused peaks can be extracted through data processing and subsequently suppressed in the ^{QD}DIPS-DARR spectrum. To address this, we have developed a data processing algorithm, as illustrated in Fig. 2, to directly extract the diagonal peaks from the ^{QD}DIPS-DARR spectrum and then completely subtract them. The process begins by taking a slice along the F1 dimension from the F2 dimension. Because any diagonal peaks are expected to appear along the zero-frequency line in the F1 dimension, this selected slice is first examined whether there exists any signal above the noise level in the spectral center. If not, the process moves onto the next F2 slice. If yes, this zero-frequency peak likely contains a diagonal peak and possible cross peaks that locate near the diagonal peak. The spin-echo refocused diagonal peak exhibits a symmetric lineshape and can be characterized by two parameters: the linewidth and the Gaussian/Lorentzian ratio. In contrast, the characteristics for any possible cross peaks, such as lineshapes and peak positions, are unknown. Thus, we do not intend to fit all peaks in the vicinity of the center of the F1 dimension. Instead, we try to extract only the diagonal peak and then subtract it from the selected slice.

The key challenge in this process is to differentiate the diagonal peak and any possible cross peaks. To address this, we simply sum the selected slice with its flipped counterpart. Since the diagonal peak is symmetric but the cross peaks shift from one side to another side upon flipping the slice, i.e., from $(\Omega_I - \Omega_S)$ to $(\Omega_S - \Omega_I)$, such a summation doubles the intensity of the symmetric diagonal peak while leaving the cross-peak intensities unchanged, provided that their linewidths at the half-height are smaller than the chemical shift separation between the cross peaks and the diagonal peak. Therefore, the diagonal peak becomes more prominent in this summed slice, allowing us to focus on the

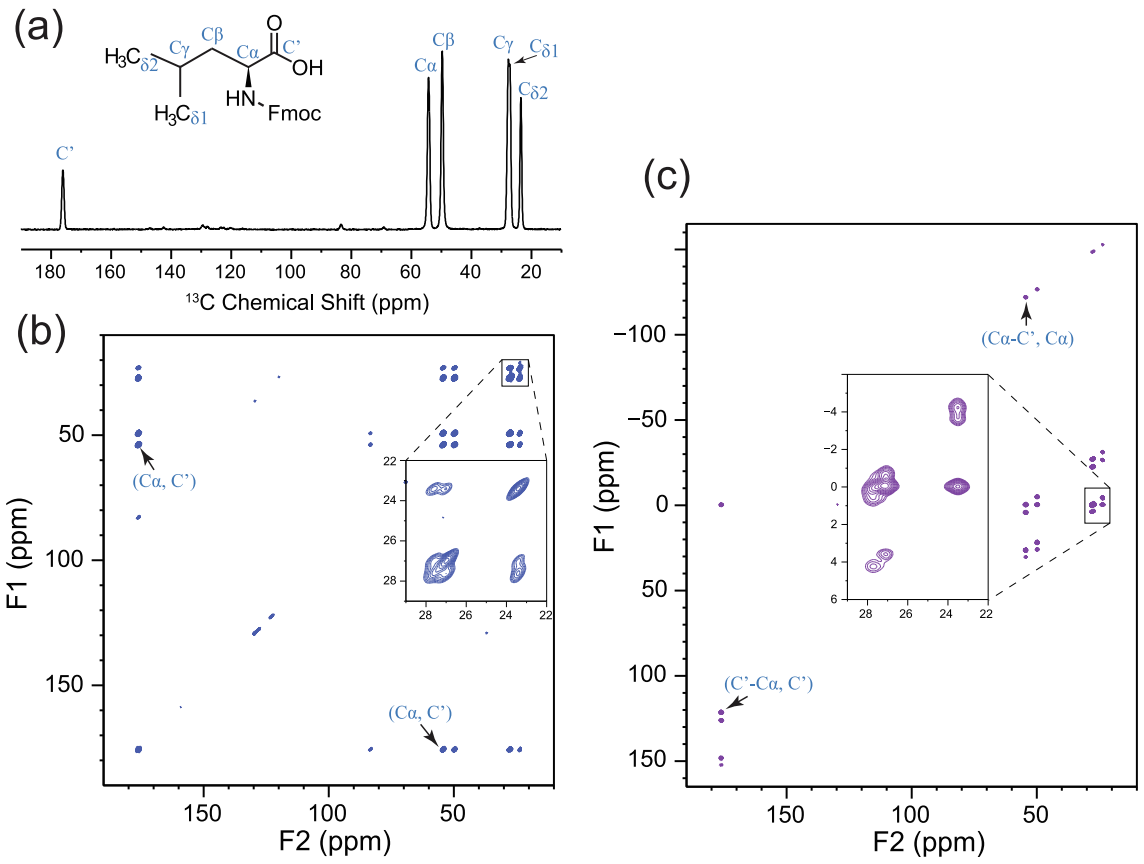

Fig. 3. (a) 1D ^{13}C CPMAS spectrum of the Fmoc-leucine sample. (b) ^{13}C–^{13}C correlation spectrum. (c) ^{QD}DIPS-DARR spectrum.

top portion of the zero-frequency peak to generate a diagonal peak through the lineshape fitting without needing to count for any underlying cross peaks. It is to note that even if the cross-peak linewidths are larger than their chemical shift separation from the diagonal peak, their intensities will only be summed partially, such that the relative intensity of the diagonal peak over the cross peaks still increases in the summed slice. In the extreme case where the cross peaks are completely overlapped with the diagonal peak, this summation does not change the relative intensities between them, which, in principle, requires a fitting that models a diagonal peak with three variables (linewidth, intensity, and Gaussian/Lorentzian ratio) and all cross peaks, each with four variables (position, linewidth, intensity, and Gaussian/Lorentzian ratio), which is highly challenging due to the unknown nature for the cross peaks. Nevertheless, as long as the diagonal peak is more intense than the cross peaks, this simplified fitting process that we propose here should still be valid.

Once the diagonal peak is extracted, we can subtract it completely from the selected slice, so that this slice contains no diagonal peak anymore. By repeating this process over the entire F2 dimension, we can obtain a ^{QD}DIPS-DARR spectrum free of diagonal peaks. Lastly, we use the same data reconstruction procedure as in [14] to transform the ^{QD}DIPS-DARR spectrum into a standard homonuclear correlation spectrum with no diagonal peaks.

3. Experimental

^{13}C labeled Fmoc-leucine was purchased from Cambridge Isotope Laboratories, Inc. and used without further purification. All NMR experiments were carried out on a Bruker Avance III 600 MHz NMR spectrometer operating at the resonance frequency of 600.13 MHz for ^{1}H and 150.82 MHz for ^{13}C using a NHMFL 3.2 mm low-E double-resonance biosolids MAS probe [17]. The sample spinning rate was controlled by a Bruker pneumatic MAS unit at 12.5 kHz ± 3 Hz. The ^{13}C magnetization was enhanced by cross-polarization (CP) with a contact time of 1 ms, during which a ^{1}H spin-lock field of 50 kHz was used and the ^{13}C B_1 field was ramped from 38 to 56 kHz. The ^{13}C 90° pulse length used was 3.0 μs. A SPINAL64 decoupling sequence [18] with a ^{1}H B_1 filed of 78.0 kHz was used during the t_1 and t_2 dimensions. During the mixing time of $t_{mixing} = 50$ ms, a ^{1}H B_1 field of 12.5 kHz was applied for the DARR irradiation to enhance the ^{13}C–^{13}C spin diffusion. The spectral widths for the t_2 and t_1 dimensions were 100 and 50 kHz, respectively. 3072 data points were acquired in the t_2 dimensions. In the t_1 dimension, 1200 points were obtained in both DARR and ^{QD}DIPS-DARR experiments so that both DARR and ^{QD}DIPS-DARR experiments has the same t_1 acquisition time. 32 scans were used in both experiments. The data were zero-filled to a 4096 × 8192 matrix before Fourier transform and no window functions were used in both dimensions in the data processing. The ^{13}C chemical shifts were referenced to the carbonyl carbon resonance of glycine at 178.4 ppm, relative to 4,4-dimethyl-4-silapentanesulfonate sodium (DSS).

4. Results and discussion

Fig. 3a shows the ^{13}C CPMAS NMR spectrum of the Fmoc-leucine sample. The isotropic chemical shifts for the six labeled ^{13}C carbons in the leucine group (i.e. C′, C_α, C_β, C_γ, $C_{\delta1}$, and $C_{\delta2}$) were uniquely assigned: $\delta_{C'} = 176.0$, $\delta_{C\alpha} = 54.2$, $\delta_{C\beta} = 49.6$, $\delta_{C\gamma} = 27.5$, $\delta_{C\delta1} = 27.1$, and $\delta_{C\delta2} = 23.4$ ppm as labeled in the spectrum. With a mixing time of t_{mixing} = 50 ms used in the experiments, spin diffusion takes place among all carbons, as shown in the ^{13}C–^{13}C correlation spectrum (c.f. Fig. 3b). For instance, the cross peaks at upper-left ($\delta_{C\alpha}$, $\delta_{C'}$) and lower-right ($\delta_{C'}$, $\delta_{C\alpha}$) correspond to the correlation between the two diagonal peak positions of C_α and C′. In particular, the protonated C_γ carbon and the methyl $C_{\delta1}$ carbon, whose chemical shifts differ only by 0.4 ppm, are differentiated

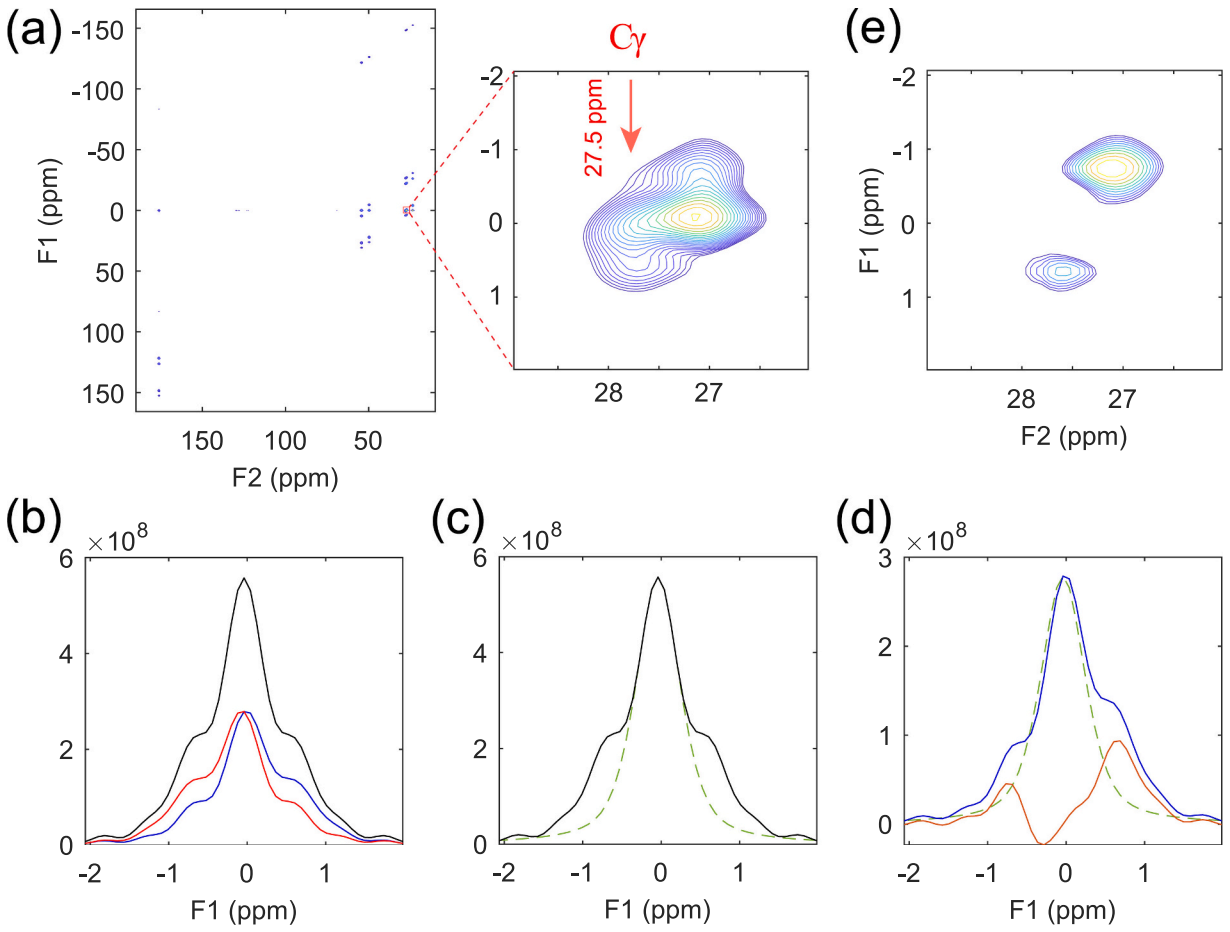

Fig. 4. (a) ^{QD}DIPS-DARR spectrum of the Fmoc-leucine sample. (b) Slice (blue) taken along 27.5 ppm, its flipped slice (red), and the sum of them (black line); (c) Diagonal peak (green dashed line) obtained though fitting the top portion of the black spectrum. (d) Subtraction of the fitted diagonal peak (green dashed line) from the selected slice (blue), resulting in diagonal peak free spectrum (red line). (e) ^{QD}DIPS-DARR spectrum after subtracting the diagonal peaks. (For interpretation of the references to colour in this figure legend, the reader is referred to the web version of this article.)

through the dipolar dephasing experiment [19], as shown in Fig. S2. The cross peaks between these two carbons appearing at ($\delta_{C\gamma}$, $\delta_{C\delta1}$) and ($\delta_{C\delta1}$, $\delta_{C\gamma}$) are so close to the diagonal axis, thus forming a typical butterfly pattern as indicated in the zoom-in spectrum.

Fig. 3c shows the 2D ^{QD}DIPS-DARR spectrum, where the cross peaks appear at their chemical shift difference positions and the autocorrelated peaks are located along the zero-frequency line, i.e., at the center in the F1 dimension. As an example, the cross peaks at ($\delta_{C\alpha}$, $\delta_{C'}$) and ($\delta_{C'}$, $\delta_{C\alpha}$) in the standard DARR spectrum (c.f., Fig. 3b) appear at ($\delta_{C'}$-$\delta_{C\alpha}$, $\delta_{C'}$) and ($\delta_{C\alpha}$-$\delta_{C'}$, $\delta_{C\alpha}$) as indicated in the ^{QD}DIPS-DARR spectrum. Since the autocorrelated peaks are the spin-echo refocused signals, they should be symmetric along the zero-frequency line as long as their cross peaks, if any, are outside the spin-echo refocused peak range. For instance, as shown in the insert of Fig. 3c, the (0, $\delta_{C\delta2}$) peak at 23.4 ppm is symmetric because the cross peak ($\delta_{C\delta2}$- $\delta_{C\delta1}$, $\delta_{C\delta2}$) is at −3.7 ppm, far away from the (0, $\delta_{C\delta2}$) peak range. However, when the cross peaks are close to the zero-frequency line, the peaks at the zero-frequency line become asymmetric. As shown in the zoom-in spectrum of Fig. 3c, due to the nearby cross peaks at ($\delta_{C\gamma}$-$\delta_{C\delta1}$, $\delta_{C\gamma}$) and ($\delta_{C\delta1}$-$\delta_{C\gamma}$, $\delta_{C\delta1}$), a small shoulder appears in the positive part of the F1 dimension along $\delta_{C\gamma}$ and in the negative part along $\delta_{C\delta1}$. Therefore, our task is to extract the symmetric diagonal peaks of (0, $\delta_{C\gamma}$) and (0, $\delta_{C\delta1}$) from these asymmetric peaks around the zero-frequency line, so that we can suppress the symmetric diagonal peaks and thus fully discover the cross peaks ($\delta_{C\gamma}$-$\delta_{C\delta1}$, $\delta_{C\gamma}$) and ($\delta_{C\delta1}$-$\delta_{C\gamma}$, $\delta_{C\delta1}$). A MATLAB program has been written to implement this data processing algorithm, as detailed in Fig. 2.

Here, we use the $\delta_{C\gamma}$ peak as an example to illustrate this process. The enlarged ^{QD}DIPS-DARR spectrum in Fig. 4a shows only the $\delta_{C\gamma}$ and $\delta_{C\delta1}$ region, where the asymmetry is apparent due to the presence of cross peaks between the two resonances. The slice taken along the $\delta_{C\gamma}$ peak at 27.5 ppm (c.f., Fig. 4a) from the ^{QD}DIPS-DARR spectrum is shown in blue in Fig. 4b, while its flipped counterpart is shown in red. Clearly the selected slice and its flipped slice differ due to the presence of the cross peak at ($\delta_{C\gamma}$-$\delta_{C\delta1}$, $\delta_{C\gamma}$). Adding them together doubles the symmetric diagonal peak but not the cross peak, making the diagonal peak more distinguishable in the summed spectrum (black in Fig. 4b) than in the selected slice (blue) taken directly from the ^{QD}DIPS-DARR spectrum. Therefore, the symmetric diagonal peak (dashed line in Fig. 4c) can be obtained by fitting the top portion of the summed spectrum with a minimum influence from the cross peaks, which are buried in the base of the summed spectrum. In general, the lineshape for the diagonal peak is comprised of Gaussian and Lorentzian components:

$$LSDP(f1) = (1-k)exp\left[\frac{-\ln(2)(f1)^2}{(LW/2)^2}\right] + (k)\frac{(LW/2)^2}{(LW/2)^2 + (f1)^2}, \quad (3)$$

where LW is the linewidth, k is the relative ratio for the Lorentzian component over Gaussian, and $f1$ represents the frequency in the F1 dimension. Both LW and k are used as the variables in the lineshape fitting. The green dashed line in Fig. 4c shows the fitted diagonal peak by fitting the top region of the zero-frequency peak in the black spectrum (the sum of the selected slice and its flipped slice) within the range from −0.89 to +0.89 ppm, about the linewidth at the half-height of the diagonal peak. This obtained diagonal peak was then scaled by 0.5 (due to

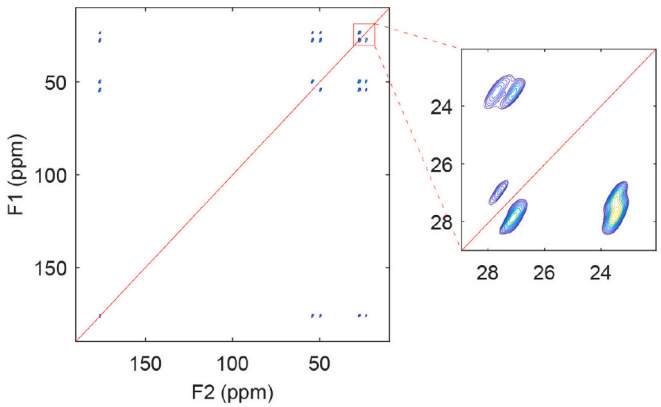

Fig. 5. Reconstructed ^{QD}DIPS-DARR spectrum of the Fmoc-leucine sample showing suppression of diagonal peaks. The diagonal axis is guided by the red lines. (For interpretation of the references to colour in this figure legend, the reader is referred to the web version of this article.)

the doubling of its intensity in the process) and then subtracted from the selected slice (blue), as shown in red in Fig. 4d. By applying this process across the entire F2 dimension, the diagonal peaks can be largely removed from the ^{QD}DIPS-DARR spectrum, as shown in Fig. 4e.

Once the diagonal peaks are removed from the ^{QD}DIPS-DARR spectrum, the standard ^{13}C–^{13}C correlation spectrum can be reconstructed using the same procedure as detailed in the reference [14]. Fig. 5 shows the reconstructed ^{QD}DIPS-DARR spectrum for the Fmoc-leucine sample, which shows the same pattern for the cross peaks but significantly less intensities for the diagonal peaks, as compared with the DARR spectrum in Fig. 3b.

Next, we applied this method to the ^{13}C,^{15}N labeled LC3B within liposomes. LC3B is a human homolog of the ubiquitin-like Atg8 protein, and its direct covalent conjugation to the amino headgroup of PE lipids in the autophagosomal membrane is a crucial step in autophagosome biogenesis during autophagy [20–23]. The LC3B-PE conjugate triggers the membrane expansion of the phagophore and serves as a marker for autophagic cargo. Here, ^{13}C,^{15}N-labeled LC3B was conjugated to PE in sonicated liposomes (POPC:DOPG:DOPE = 3:2:5, molar ratio) using an E1-like mouse Atg7 and an E2-like human Atg3 enzymes. Details about

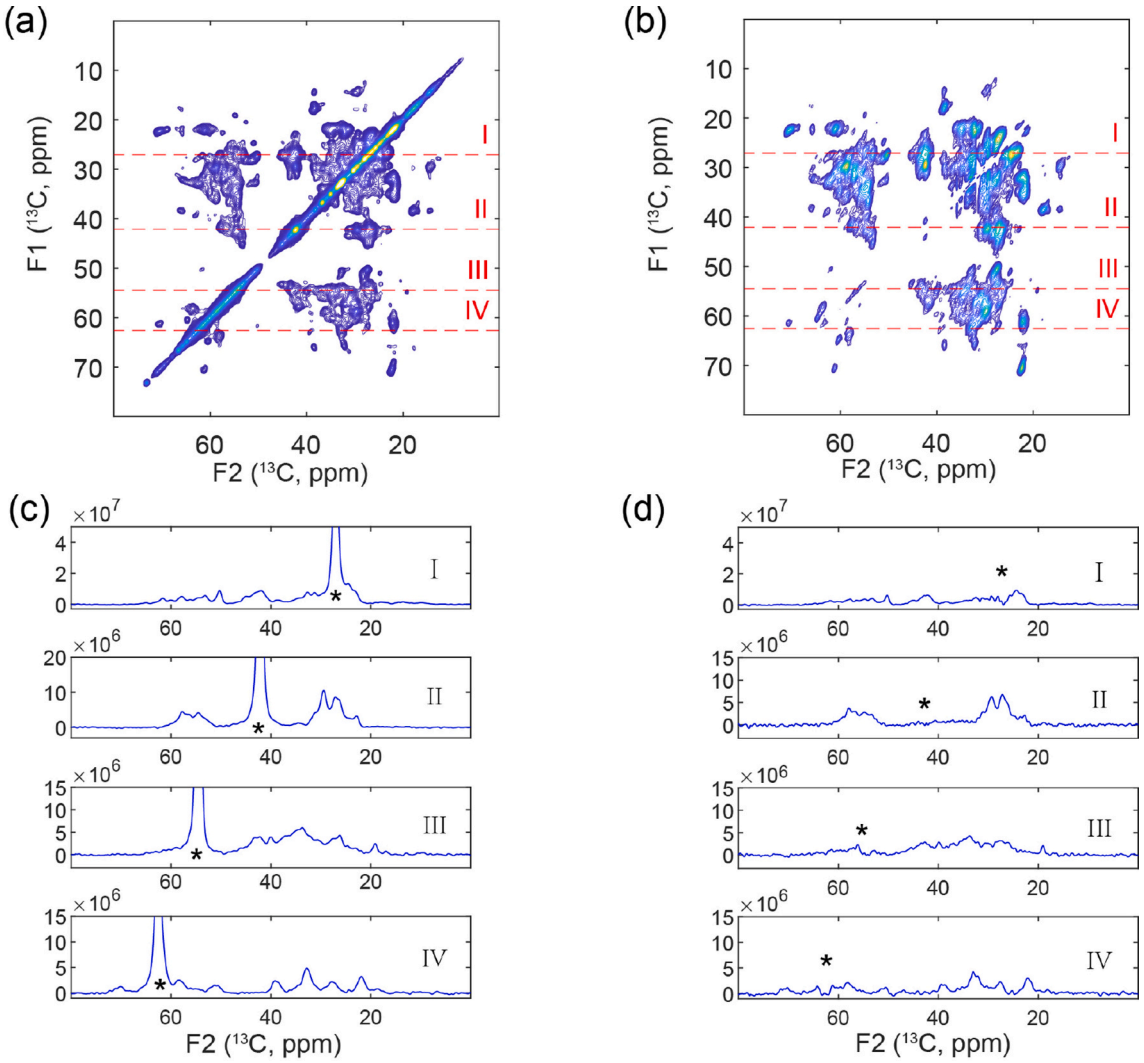

Fig. 6. Experimental results of ^{13}C,^{15}N-labeled LC3B-PE in liposomes. (a) The standard DARR spectrum. (b) The reconstructed ^{QD}DIPS-DARR spectrum. (c) Slices taken along the red dashed lines indicated in the spectra. Both the standard DARR and ^{QD}DIPS-DARR spectra were recorded on a Bruker Avance III 600 MHz NMR spectrometer. The sample spinning rate was 12.5 kHz. The CP condition was the same as in Fig. 3. 128 scans were used to accumulate each of 1024 t_1 increment. A 20 ms mixing time was used in both experiments. A Gaussian window function (LB = −30 Hz and GB = 0.1) was applied in both dimensions during the data processing. The asterisk in the slices indicate the positions of the diagonal peaks. (For interpretation of the references to colour in this figure legend, the reader is referred to the web version of this article.)

the sample preparation, including protein expression and purification, are given in the Supplemental Material. The conjugated ^{13}C,^{15}N-labeled LC3B-PE in liposomes was subsequently packed into a rotor for solid-state NMR analysis. Fig. 6 shows the ^{13}C–^{13}C correlation spectra of the ^{13}C,^{15}N-labeled LC3B-PE in liposomes. In the standard DARR spectrum in Fig. 6a, the strong diagonal peaks from the ^{13}C-labeled proteins, as well as from natural abundance lipids, obscure cross peaks that are close to the diagonal axis, particularly in the sidechain carbon region between 20 and 40 ppm and in the C_α region. For comparison, in the reconstructed ^{QD}DIPS-DARR spectrum (c.f., Fig. 6b) the resonance patterns away from the diagonal axis remain the same, while almost no diagonal peaks are present along the diagonal axis. As a result, cross-peaks that are close to the diagonal axis can now be readily identified. Slices taken from the DARR and reconstructed ^{QD}DIPS-DARR spectra further illustrate that the strong diagonal peaks (indicated by the asterisks in Fig. 6c) in the DARR spectrum are markedly reduced in the reconstructed ^{QD}DIPS-DARR spectrum (c.f. Fig. 6d), while the off-diagonal peaks (i.e., the cross peaks) remain the same. It is to note that the cross-peak intensities in the reconstructed ^{QD}DIPS-DARR spectrum appear to be lower than those in the DARR spectrum. As an example, the signal-to-noise ratio for the cross peak at (62.4, 70.7) ppm was measured to be 15.2 and 7.6, respectively, from the standard DARR spectrum in Fig. 6a and from the reconstructed ^{QD}DIPS-DARR spectrum in Fig. 6b. This occurs because only 50 % of the spin-diffused signals remain in the sine and cosine modulations of the chemical shift differences in this spin-echo based diagonal peak suppression method, as indicated in Eqs. (7) and (14) in the Supplemental Material. Additionally, since the ^{QD}DIPS-DARR scheme uses two t_1 evolution periods, signals with unfavorable T_2* relaxation time may experience further reduction in the signal-to-noise ratio as compared to the standard DARR experiments.

It is to note that any pulse imperfections, offset effects, and instrumentation instability might produce artifacts or cause t_1-noises in the F1 dimension, as this proposed ^{QD}DIPS-DARR scheme uses a complete set of phase cycling steps to select the sine/cosine modulations in the t_1 dimension by canceling out many other unwanted signals. However, any artifacts or t_1-noises should have limited impacts on the proposed diagonal peak extraction algorithm. This is because adding a slice and its flipped counterpart preserves the symmetry of a zero-frequency peak while enhancing the signal-to-noise ratio relative to any t_1-noises. As a result, the diagonal peak can be reliably extracted and subsequently suppressed using our proposed fitting procedure. Furthermore, any t_1-noises in the reconstructed ^{QD}DIPS-DARR spectrum could be suppressed through additional symmetric operation, similar to the method used in solution NMR [24,25]. Although such a symmetric operation is not common in solid-state NMR chemical shift correlation spectra, it offers a potential means for suppression of artifacts.

5. Conclusion

The quadrature detected spin-echo based diagonal peak suppression method, i.e., ^{QD}DIPS-DARR, has been proposed in high-resolution solid-state MAS NMR homonuclear chemical shift correlation experiments. A comprehensive phase cycling is designed to select the sine and cosine modulations of the chemical shift difference between the spin-diffused signals in the indirect dimension, allowing for quadrature detection through the hypercomplex method. Signals that do not participate in polarization transfers do not evolve in the indirect dimension and thus appear at the center of the indirect dimension. Furthermore, a post-data processing algorithm has been developed to extract the lineshapes of these spin-echo refocused signals and remove them from the center of the indirect dimension. The reconstruction of the resulting spectrum yields a conventional-like homonuclear correlation spectrum free of diagonal peaks. Experimental results demonstrate that over 99 % of the diagonal peak intensities could be suppressed, while approximately 50 % of the cross-peak intensities remain in the reconstructed ^{QD}DIPS-DARR spectrum, with possibly further decrease due to the doubling of the t_1 evolution time. Nevertheless, this efficient diagonal peak suppression method offers the potential to identify cross-peaks close to the diagonal axis, such as between C_α resonances and between aliphatic carbons from different residues in proteins, in homonuclear chemical shift correlation spectra. This will be beneficial for resonance assignments and structural characterizations [26,27].

CRediT authorship contribution statement

Shengyu Zhang: Writing – original draft, Software, Methodology, Formal analysis. **Yuchen Li:** Writing – original draft, Software, Methodology, Formal analysis. **Yansheng Ye:** Writing – review & editing, Data curation. **Fang Tian:** Writing – review & editing, Writing – original draft, Resources, Data curation. **Xinhua Peng:** Writing – review & editing, Writing – original draft, Conceptualization. **Riqiang Fu:** Writing – review & editing, Writing – original draft, Methodology, Formal analysis, Data curation, Conceptualization.

Declaration of competing interest

The authors declare that they have no known competing financial interests or personal relationships that could have appeared to influence the work reported in this paper.

Acknowledgements

All NMR experiments were carried out at the National High Magnetic Field Lab (NHMFL) supported by the NSF Cooperative Agreement DMR-2128556 and the State of Florida. F.T. acknowledges the support from the National Institutes of Health through R01 GM127730. X.P. acknowledges the support from Innovation Program for Quantum Science and Technology through 2021ZD0303205, National Natural Science Foundation of China through No. 12261160569, and the XPLORER Prize.

Appendix A. Supplementary data

Supplementary data to this article can be found online at https://doi.org/10.1016/j.jmr.2025.107926.

Data availability

Data and MATLAB code will be made available upon request.

References

[1] S. Glanzer, E. Schrank, K. Zangger, A general method for diagonal peak suppression in homonuclear correlated NMR spectra by spatially and frequency selective pulses, J. Magn. Reson. 232 (2013) 1–6.
[2] G.S. Harbison, J. Feigon, D.J. Ruben, J. Herzfeld, R.G. Griffin, Diagonal peak suppression in 2D-NOE spectra, J. Am. Chem. Soc. 107 (1985) 5567–5569.
[3] J.J. Lopez, C. Kaiser, S. Shastri, C. Glaubitz, Double quantum filtering homonuclear MAS NMR correlation spectra: a tool for membrane protein studies, J. Biomol. NMR 41 (2008) 97–104.
[4] M. Hong, Solid-state dipolar INADEQUATE NMR spectroscopy with a large double-quantum spectral width, J. Magn. Reson. 136 (1999) 86–91.
[5] D. Huster, L. Xiao, M. Hong, Solid-state NMR investigation of the dynamics of the soluble and membrane-bound colicin Ia channel-forming domain, Biochemistry 40 (2001) 7662–7674.
[6] R. Verel, M. Ernst, B.H. Meier, Adiabatic dipolar recoupling in solid-state NMR: the DREAM scheme, J. Magn. Reson. 150 (2001) 81–99.
[7] J. Keeler, Understanding NMR Spectroscopy, 2nd ed., Wiley, 2010.
[8] N. Bloembergen, S. Shapiro, P.S. Pershan, J.O. Artman, Cross-relaxation in spin systems, Phys. Rev. 114 (1959) 445–459.
[9] K. Takegoshi, S. Nakamura, T. Terao, 13C–1H dipolar-assisted rotational resonance in magic-angle spinning NMR, Chem. Phys. Lett. 344 (2001) 631–637.
[10] M. Weingarth, D.E. Demco, G. Bodenhausen, P. Tekely, Improved magnetization transfer in solid-state NMR with fast magic angle spinning, Chem. Phys. Lett. 469 (2009) 342–348.
[11] Y. Wei, A. Ramamoorthy, 2D 15N–15N isotropic chemical shift correlation established by 1H–1H dipolar coherence transfer in biological solids, Chem. Phys. Lett. 342 (2001) 312–316.

[12] K. Xue, T.K. Movellan, L.B. Andreas, Orphan spin operator diagonal suppression, J. Magn. Reson. Open 10–11 (2022) 100025.
[13] A. Banerjee, N. Chandrakumar, Two-dimensional nuclear magnetic resonance: exploiting spin echoes to maximize information content by suppression of diagonal peaks in homonuclear experiments, Chem. Eur. J. 119 (2015) 482–487.
[14] K.Y. Wang, Z.Y. Zhang, X.Y. Ding, F. Tian, Y.Q. Huang, Z. Chen, R. Fu, Spin-echo based diagonal peak suppression in solid-state MAS NMR homonuclear chemical shift correlation spectra, J. Magn. Reson. 287 (2018) 91–98.
[15] Z. Zhang, H. Chen, C. Wu, R. Wu, S. Cai, Z. Chen, Spatially encoded ultrafast high-resolution 2D homonuclear correlation spectroscopy in inhomogeneous fields, J. Magn. Reson. 227 (2013) 39–45.
[16] K. Takegoshi, S. Nakamura, T. Terao, 13C–1H dipolar-driven 13C–13C recoupling without 13C rf irradiation in nuclear magnetic resonance of rotating solids, J. Chem. Phys. 118 (2003) 2325–2341.
[17] P.L. Gor'kov, E.Y. Chekmenev, C. Li, M. Cotten, J.J. Buffy, N.J. Traaseth, G. Veglia, W.W. Brey, Using low-E resonators to reduce RF heating in biological samples for static solid-state NMR up to 900MHz, J. Magn. Reson. 185 (2007) 77–93.
[18] B.M. Fung, A.K. Khitrin, K. Ermolaev, An improved broadband decoupling sequence for liquid crystals and solids, J. Magn. Reson. 142 (2000) 97–101.
[19] S. Dugar, R. Fu, N.S. Dalal, Increasing ^{13}C CP-MAS NMR resolution using single crystals: application to model octaethyl porphyrins, J. Phys. Chem. B 116 (2012) 9215–9222.
[20] Z. Yang, D.J. Klionsky, An overview of the molecular mechanism of autophagy, Curr. Top. Microbiol. Immunol. 335 (2009) 1–32.
[21] N. Mizushima, T. Yoshimori, Y. Ohsumi, The role of Atg proteins in autophagosome formation, Annu. Rev. Cell Dev. Biol. 27 (2011) 107–132.
[22] D.J. Klionsky, B.A. Schulman, Dynamic regulation of macroautophagy by distinctive ubiquitin-like proteins, Nat. Struct. Mol. Biol. 21 (2014) 336–345.
[23] Y.S. Ye, E.R. Tyndall, V. Bui, Z.Y. Tang, Y. Shen, X.J. Jiang, J.M. Flanagan, H. G. Wang, F. Tian, An N-terminal conserved region in human Atg3 couples membrane curvature sensitivity to conjugase activity during autophagy, Nat. Commun. 12 (2021) 374.
[24] G. Wider, S. Macura, R.R. Ernst, K. Wuthrich, Homonuclear two-dimensional ^{1}H NMR of proteins. Experimental procedures, J. Magn. Reson. 56 (1984) 207–234.
[25] R.R. Ernst, G. Bodenhausen, A. Wokaun, Principles of Nuclear Magnetic Resonance in One and Two Dimensions, Clarendon Press, Oxford, 1987.
[26] Y. Shin, R. Prasad, N. Das, J.A. Taylor, H. Qin, W.H. Hu, Y.Y. Hu, R. Fu, R. Zhang, H.X. Zhou, T.A. Cross, *Mycobacterium tuberculosis* CrgA forms a dimeric structure with its transmembrane domain sandwiched between cytoplasmic and periplasmic β-sheets, enabling multiple interactions with other divisome proteins, J. Am. Chem. Soc. 147 (2025) 11117–11131.
[27] A. Ramamoorthy, J. Xu, 2D ^{1}H/^{1}H RFDR and NOESY NMR experiments on a membrane-bound antimicrobial peptide under magic angle spinning, J. Phys. Chem. B 117 (2013) 6693–6700.